IEICE Proceeding Series

Read and Write Operations of Memory Device Consisting of Nonlinear MEMS Resonator

Atsushi YAO, Takashi HIKIHARA

Vol. 1 pp. 352-355
Publication Date: 2014/03/17
Online ISSN: 2188-5079

2012 International Symposium on Nonlinear Theory and its Applications
NOLTA2012, Palma, Majorca, Spain, October 22-26, 2012

Read and Write Operations of Memory Device Consisting of Nonlinear MEMS Resonator

Atsushi YAO† and Takashi HIKIHARA‡

Department of Electrical Engineering, Kyoto University
Katsura, Nishikyo, Kyoto, 615-8510 Japan
Email: †yao@dove.kuee.kyoto-u.ac.jp, ‡hikihara.takashi.2n@kyoto-u.ac.jp

Abstract—Nonlinear MEMS resonator exhibits two stable periodic vibrations with hysteresis at a single excitation frequency. Badzey *et al.* reported that the nonlinear MEMS resonator can be applied to a memory device. Based on their results, we try to demonstrate read and write operations of the memory device. In this paper, the read out operation of the device is achieved via a current through capacitor which is proportional to the displacement of MEMS resonator in differential configuration. Through the experiments and numerical simulations, the write operation is also performed by a displacement feedback control.

1. Introduction

Micro-electro-mechanical systems (MEMS) devices contain both electrical and mechanical components at the micron-scale dimensions [1]. Among many MEMS devices, we focus on MEMS resonators which have been studied as sensor elements, filters, and frequency references [1]. Because of hardening nonlinear stiffness, MEMS resonators are known to have nonlinear frequency responses at large amplitude excitation [1, 2]. MEMS resonators exhibit hysteresis characteristics at an up and down sweep of frequency and have two stable vibrating states at a single frequency in the hysteresis region [1, 2]. Badzey *et al.* indicated that these nonlinear MEMS resonators can be used as a mechanical 1 bit memory device [3]. Based on their results, we study read and write operations of the memory device.

The memory device consisting of MEMS resonator has two advantages. One is the power consumption of the device. It becomes principally lower than CMOS-based memories when it is fabricated in nano-electromechanical systems technology [4, 5]. The other is the possibility to develop an active MEMS memory. It allows parallel logic circuits in a single mechanical resonator [5].

For the memory device in micro- and nano-electromechanical resonators [3, 4, 6, 7], the write operation corresponds to a switching of two stable periodic vibrations. Recently, Unterreithmeier *et al.* discussed a switching between two coexisting stable states in a nonlinear MEMS resonator at a fixed excitation frequency [7]. They applied a radio-frequency pulse to bring one stable state to the other. Their results motivated us to find other appropriate continuous control methods for the practical use based on feedback control. Through the experiments and numerical simulations, it is found that the switching is achieved between two coexisting stable states by a displacement feedback control.

On the other hand, for the displacement feedback control, the real-time displacement measurement is required. We propose the measurement by a self-sensing method for the combined structure of actuator and sensor in a MEMS resonator. The self-sensing can be a solution for the integration and the simplification of whole system [8, 9]. From this standpoint, we confirm a self-sensing method as a measurement of the current through capacitor which is proportional to the displacement of MEMS resonator. The displacement measurement also implies the read operation of memory device.

The overview of this paper is organized as follows. In Sec. 2, a fabricated MEMS resonator is presented. Sec. 3 explains the details of the displacement measurement as the read operation in the MEMS resonator. In Sec. 4, we introduce the switching control as the write operation. Sec. 5 summarizes this paper.

2. MEMS resonator

As for a MEMS resonator, a comb-drive resonator is designed and fabricated to obtain hysteretic characteristics during the up and down sweep of frequency as shown in Fig. 1 [10, 11]. Fig. 1 shows a perforated mass suspended by springs, which are connected to anchor [10, 11]. When the MEMS resonator is excited, the mass vibrates only in x-direction.

When the mass vibrates, the capacitance changes with relations

$$C_1 = 2\varepsilon N \frac{h(l+x)}{d},\ C_2 = 2\varepsilon N \frac{h(l-x)}{d}, \qquad (1)$$

where C_1 denotes the capacitance of the right electrode, C_2 the capacitance of the left electrode, x the displacement, d ($= 3$ μm) the gap between the fingers, l ($= 100$ μm) the initial overlap between the fingers, ε ($= 8.8541 \times 10^{-12}$ F/m) the permittivity, N ($= 39$)

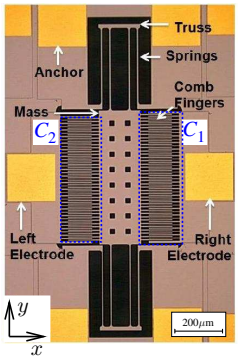

Figure 1: Schematic diagram of fabricated MEMS resonator.

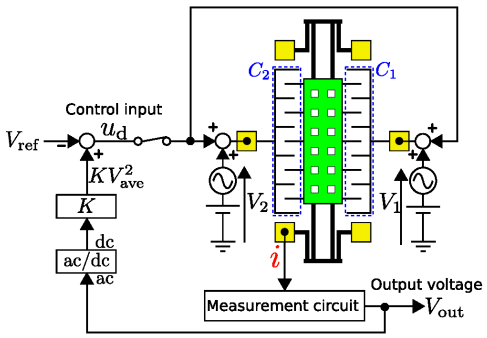

Figure 2: Switching and measurement system.

the comb number, and h ($= 25$ μm) the finger height.

3. Read operation

In this section, we explain a displacement measurement of comb-drive resonator by using the differential measurement [12] as the read operation of memory device consisting of the nonlinear MEMS resonator.

In the measurement, the excitation force F is obtained by the following equations:

$$\begin{aligned} F &= \left(\frac{\partial C_1}{\partial x}\right)\frac{V_1^2}{2} + \left(\frac{\partial C_2}{\partial x}\right)\frac{V_2^2}{2} \\ &= 4\varepsilon N\frac{h}{d}V_{\rm dc}v_{\rm ac}\sin 2\pi ft, \end{aligned} \tag{2}$$

where V_1 ($= V_{\rm dc} + v_{\rm ac}\sin 2\pi ft$) denotes the applied voltage to the right electrode, V_2 ($= V_{\rm dc} - v_{\rm ac}\sin 2\pi ft$) the applied voltage to the left electrode, and f the excitation frequency. In the experiments, the dc bias voltage $V_{\rm dc}$ and the ac excitation amplitude $v_{\rm ac}$ are set at -0.15 V and 0.7 V in room temperature with a vacuum at 10 Pa.

The sum of the current through the right and left capacitor i is converted to the output voltage $V_{\rm out}$ by two operational amplifiers. The first stage operational amplifier works as the current-to-voltage (I-V) converter

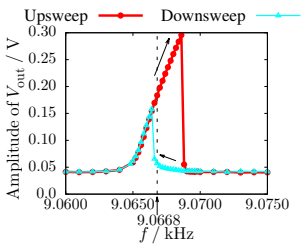

(a) Frequency response curve.

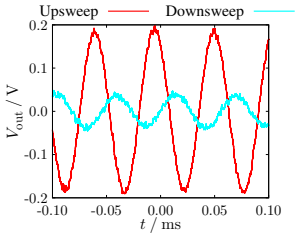

(b) Oscillogram of two stable periodic vibrations at 9.0668 kHz.

Figure 3: Displacement measurement by differential configuration (experimental results).

and the second as the inverting amplifier. When the displacement $x(t)$ is assumed as $A_0\sin(2\pi ft + \phi)$, the output voltage $V_{\rm out}$ becomes

$$\begin{aligned} V_{\rm out} &= R\frac{R_2}{R_1}i = R\frac{R_2}{R_1}\left(\frac{\partial(C_1V_1)}{\partial t} + \frac{\partial(C_2V_2)}{\partial t}\right) \\ &= 8\pi fR\frac{R_2}{R_1}\varepsilon N\frac{h}{d}v_{\rm ac}A_0\sin(4\pi ft + \phi), \end{aligned} \tag{3}$$

where A_0 and ϕ denote the amplitude and the phase of the displacement. The resistors R, R_1, and R_2 are set at 1 MΩ, 1 kΩ, and 100 kΩ, respectively. We can confirm that $V_{\rm out}$ depends on both the amplitude A_0 and the phase ϕ of the displacement x. The frequency of the output voltage becomes twice to the excitation frequency f.

Figure 3(a) depicts the experimentally obtained frequency response curve of $V_{\rm out}$. The red and aqua lines show the response at the up and down sweep of frequency, respectively. It was found that the MEMS resonator has hysteresis characteristics to frequency and two stable states coexist in the hysteresis.

Figure 3(b) shows the oscillogram of two stable periodic vibrations at 9.0668 kHz. In Fig. 3(b), the red and aqua lines are obtained by the average of 16 times measurements. We confirmed that the amplitude and the phase of these vibrations are obviously distinguished. In the following experiments, the excitation frequency is fixed at 9.0668 kHz.

4. Write operation

In this section, we discuss the switching operation between two coexisting states as the write operation of memory device. The results in Sec. 3 provided that the fabricated MEMS resonator has two stable periodic vibrations. When we consider the set of initial conditions sampled by the period of the periodic excitation, the basins of attraction for the two stable solutions are completely separated by stable manifolds for an unstable solution [13]. We aim for smooth switching between two stable periodic vibrations at a fixed excitation frequency.

4.1. Experimental result

Here, the switching operation between two coexisting states is experimentally discussed by a displacement feedback control at a fixed excitation frequency. The feedback control is based on the output voltage, which is returned as a proportional signal to the displacement (see Fig. 2). However, the control input must avoid the influence to measurement. It should be noted that the excitation force F depends on both the ac and dc voltages but the output voltage $V_{\rm out}$ does not on the dc voltage as in Eqs. (2) and (3). The feature makes it possible that the control input is applied as a slowly changed dc voltage to MEMS resonator.

Figure 2 is the proposed switching system between two vibrations by the displacement feedback control to the MEMS resonator. The output ac voltage $V_{\rm out}$ is converted to the square average dc voltage $V_{\rm ave}^2$ by an analog multiplier and a low pass filter of the operational amplifier.

The control input $u_{\rm d}$ is given as a slowly changed dc voltage by

$$u_{\rm d} \quad = \quad -V_{\rm ref} + KV_{\rm ave}^2, \tag{4}$$

where K denotes the feedback gain and $V_{\rm ref}$ the external reference signal. The external reference signal is set as $K|V_{\rm out}^{\rm L}|^2$ and $K|V_{\rm out}^{\rm S}|^2$ when the state is requested to switch to the large and small amplitude vibration, respectively. Here, $V_{\rm out}^L$ and $V_{\rm out}^S$ correspond to the targeted output voltage for the large and small amplitude vibrations. The feedback gain is set at 5.1. As a result, the excitation force F is given with the control input $u_{\rm d}$ by

$$F \quad = \quad 4\varepsilon N\frac{h}{d}(V_{\rm dc}+u_{\rm d})v_{\rm ac}\sin 2\pi ft. \tag{5}$$

Figures 4(a) and 4(b) show the vibrations switched by the feedback input $u_{\rm d}$. In these figures, aqua and purple lines correspond to the output voltage $V_{\rm out}$ and the control input $u_{\rm d}$, respectively. The control input was applied at 1 s from the beginning of the oscillogram. Figs. 4(a) and 4(b) show the result of the switching from small to large amplitude vibrations and from large to small, respectively. In Figs. 4(a) and 4(b), it was observed that the state converged to small and large amplitude periodic vibrations in the comb-drive resonator, respectively. After the switching was completed, the control input $u_{\rm d}$ became null.

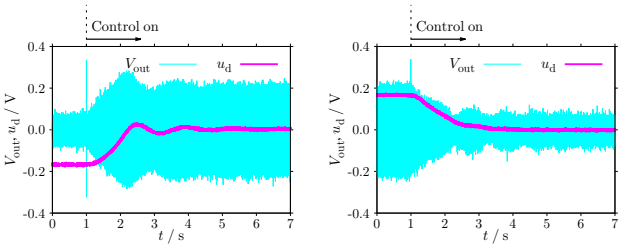

(a) Switching from small to large amplitude vibration.

(b) Switching from large to small amplitude vibration.

Figure 4: Switching between two stable periodic vibrations (experimental results).

4.2. Numerical result

It was shown that a MEMS resonator can be a dynamic memory device. For the write operation, the memory device exhibits the convergence to the steady state experimentally. Here, we discuss the transient behavior using numerical simulations at the low noise condition in the measurement and the switching.

The motion of the MEMS resonator with nonlinearity is given by the following non-dimensional differential equations [14]:

$$\begin{cases} \dfrac{{\rm d}x}{{\rm d}t} = y, \\ \dfrac{{\rm d}y}{{\rm d}t} = -\dfrac{y}{Q} - x - \alpha_3 x^3 + (k_{\rm e}+u)\sin\omega t, \end{cases} \tag{6}$$

where x denotes the resonator displacement, y the displacement velocity, u the control signal, ω (= 1.02) the excitation frequency, Q (= 282) the quality factor, α_3 (= 3.23) the coefficient of cubic correction to the linear restoring force, and $k_{\rm e}$ (= 0.001) the amplitude of the excitation force. The parameter settings are due to Ref. [14] because the same device is assigned as shown in Fig. 1. Fig. 5 shows the simulated frequency response curve of the resonator, which has two stable solutions and an unstable solution.

According to the experimental method, the control signal u is given as the following equations:

$$u \quad = \quad K^*(A_{\rm ref}^2 - A_{\rm ave}^2), \tag{7}$$

$$A_{\rm ave}^2 \quad = \quad \frac{A_1^2 + A_2^2 + \cdots + A_m^2 + \cdots + A_M^2}{M}, \tag{8}$$

where K^* denotes the feedback gain, $A_{\rm ref}$ the external reference signal of amplitude, m natural number, M the average number, and A_m the displacement amplitude of the previous m period within $1 \le m \le M$. Then, $A_{\rm ave}^2$ is the average of A_m^2. We set K^* at 0.05 and so do M at 100. When the state is switched to the large and small amplitude vibration, the external reference signal $A_{\rm ref}$ is set at $(A_{\rm out}^{\rm L})^2$ and $(A_{\rm out}^{\rm S})^2$, respectively. Here, $A_{\rm out}^L$ and $A_{\rm out}^S$ show the target of amplitude to the large and small vibrations.

Figures 6(a) and 6(b) depict the time evolution from small to large vibration and from large to small, respectively. In these figures, the purple and aqua plots correspond to the control signal and the displacement, respectively. We can find the similarity of numerical results in Figs. 6(a) and 6(b) to experiments in Fig. 4.

Figure 6(c) shows the obtained trajectories in the phase space. In the figure, the white and black regions

show the basins of two stable solutions [15] without control signal in Eq. (6). Every initial state obviously corresponds to the convergence to small (white) and large (black) amplitude solutions. The aqua and red points imply the loci of stroboscopic states from small and large vibrations, respectively. It should be noted that the states slowly transfer from small to large amplitude solutions and from large to small. These loci of stroboscopic states appear along unstable manifolds of an unstable saddle. Therefore, the feedback gain should be enough for the loci of stroboscopic states to pass across the unstable manifolds. Fig. 6(c) shows that there exist the points of intersection of these loci. The active MEMS memory may allow the rewrite operation when the vibrating state is the transient state near these points. It will be a new research target. We are currently investigating the detail transient behavior.

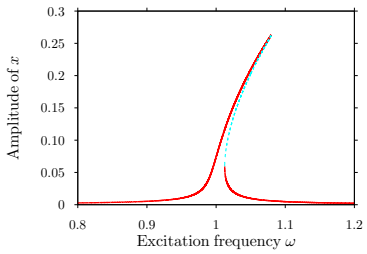

Figure 5: Frequency response curve (numerical result). The red lines show two stable solutions and the blue line an unstable solution.

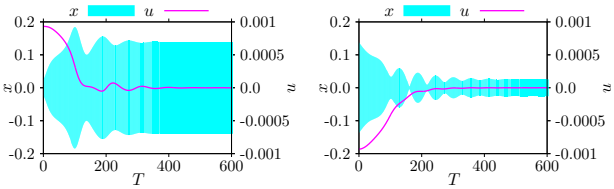

(a) Time evolution of switching from small to large amplitude vibration.

(b) Time evolution of switching from large to small amplitude vibration.

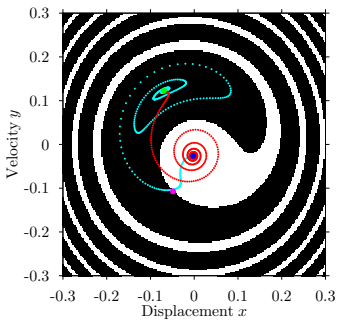

(c) Trajectories under control in phase space. The green point shows the large amplitude solution and the blue the small solution without control signal.

Figure 6: Switching between two stable periodic vibrations (numerical results).

5. Concluding remarks

This paper experimentally realized the read and the write operations of the memory device consisting of the nonlinear MEMS resonator by the self-sensing method and the displacement feedback control. Furthermore, the transient behavior was numerically investigated in the write operation. As a result, we confirmed the requirement of the feedback gain and the possibility of the rewrite function. The controlled transition of the state of device will give us another possible design of memory at their active operation.

Acknowledgments

We would like to show our appreciation to Dr. S. Naik, SPAWAR, USA, who was the previous Ph. D. students of Kyoto University, for the discussion about the design of MEMS resonator. This research was partially supported by Global COE of Kyoto University, Regional Innovation Cluster Program "Kyoto Environmental Nanotechnology Cluster", and JSPS KAKENHI (Grant-in-Aid for Exploratory Research) ♯21656074.

References

[1] V. Kaajakari, "Practical MEMS," Small Gear Publishing, 2009.

[2] A. Frangi *et al.*, "Advances in Multiphysics Simulation and Experimental Testing of MEMS," Imperial College Press, 2008.

[3] R. L. Badzey *et al.*, *Applied Physics Letters*, vol. 85, no. 16, pp. 3587–3589, 2004.

[4] I. Mahboob and H. Yamaguchi, *Nature nanotechnology*, vol. 3, no. 5, pp. 275–279, 2008.

[5] I. Mahboob *et al.*, *Nature Communications*, vol. 2, no. 1201, 2011.

[6] H. Noh *et al.*, *Applied Physics Letters*, vol. 97, no. 3, pp. 033116-1–033116-3, 2010.

[7] Q. P. Unterreithmeier *et al.*, *Physical Review B*, vol. 81, no. 24, pp. 241405-1–241405-4, 2010.

[8] I. A. Ivan *et al.*, *Review of Scientific Instruments*, vol. 80, no. 6, pp. 065102-1–065102-8, 2009.

[9] K. Matsuda *et al.*, *Transactions of the Japan Society of Mechanical Engineers. C*, vol. 63, no. 609, pp. 1441–1447, 1997. (in Japanese)

[10] S. Naik and T. Hikihara, *IEICE Electronics Express*, vol. 8, no. 5, pp. 291–298, 2011.

[11] S. Naik, "Investigation of synchronization in a ring of coupled MEMS resonators," Doctoral Dissertation (Kyoto University), 2011.

[12] V. Kempe, "Inertial MEMS: Principles and Practice," Cambridge University Press, 2011.

[13] Y. Ueda, "Theory of Chaotic Phenomena," Korona, 2008. (in Japanese)

[14] S. Naik *et al.*, *Journal of Sound and Vibration*, vol. 331, no. 5, pp 1127–1142, 2012.

[15] J. Guckenheimer and P. Holmes, "Nonlinear Oscillations, Dynamical Systems, and Bifurcations of Vector Fields," Springer-Verlag, 1983.